An Elaborate Seismic Study of Beirut: Integrating 3D Multidisciplinary Geotechnical Model Definition, Machine Learning Enhancements, and Numerical Simulations

Marwa Safa[1, 2#], *Etienne* Bertrand[1], *Marleine* Brax[2], *and Rafael* Abreu[3]

[1] *Gustave Eiffel University, GERS-SRO, 14-20 bvd Newton, 77420 Champs-sur-Marne, France*
[2] *CNRS-L, National Center for Geophysical Research, Bhannes, Lebanon*
[3] *Paris Cité University,IPGP, 1 rue Jussieu, 75005 Paris, France*

[#]*Corresponding author: safa.marwa@univ-eiffel.fr*

ABSTRACT

In seismic hazard assessment, reliance on Vs30 proxies and 1D shear wave velocity profiles often leads to underestimated ground motion. This is particularly evident in areas with complex geological structures, such as Greater Beirut (GB). The metropolis, situated near active seismic faults, experienced significant nearby earthquakes in 551, 1202, and 1837. It is characterized by diverse soil compositions, that vary from sandy terrains to limestone formations, demanding a detailed geotechnical model for seismic hazard studies. Our research developed a comprehensive 3D geotechnical model for GB, integrating data from around 500 boreholes, 700 geophysical measurements, refined DEM, and geological insights. The model delineates variations in bedrock elevation and geological strata, some sites exhibiting sediment depths up to 80 meters. We performed an iterative data analysis by combining the horizontal to vertical spectral ratio method (H/V measurements) with borehole data. This approach enabled us to estimate the average shear wave velocity (Vs-mean) in the sedimentary layer and the depth of the bedrock across the model. To address data gaps in southern GB, we used a Random Forest machine learning model, trained on interpolated points from Kriging in the central model part, ensuring continuous representation of sedimentary units even in data-limited areas. Ongoing work involves seismic simulations predicting ground motion amplification in Beirut. Using a 3D hexahedral mesh generated via Python code, we will conduct full 3D numerical simulations of seismic wave propagation. These simulations aim to provide insights into Beirut's seismic response, contributing to earthquake preparedness and risk mitigation. We will present preliminary results in predicting the seismic motion in Greater Beirut using SPECFEM3D, a spectral-element method software designed for 3D seismic wave propagation simulations.

Keywords: 3D Geotechnical Modeling, Greater Beirut, Seismic Hazard Assessment, SPECFEM3D Simulations, Hexahedral mesh

1. Introduction

The city of Beirut, capital of Lebanon, situated on a peninsula at the midpoint of Lebanon's Mediterranean coast, has been damaged several times by historical earthquakes (e.g., the 551 A.D off-shore event is the most devastating earthquake for the city which was of magnitude exceeding 7; moreover it was accompanied by a tsunami that affected the whole coast from North to South of Lebanon and resulted in more than 30,000 deaths). Beirut is located on the 1,200 km transforming fault system known as the Levant fault system, with its population reaching more than 2.5 million inhabitants and a significant increase in the construction of buildings in the last years. Consequently, damages from future earthquakes in Beirut could have a huge effect on the whole country. The estimation of the potential seismic strong ground motion, including local site effects, is of great importance for Greater Beirut (GB).

The knowledge of subsoil layers of GB is still not well constrain and its influence on the seismic ground motion in the area needs to be investigated. For instance, the depth of the bedrock which underlays the quaternary deposits is not well known and the stratigraphy in the quaternary deposits is not yet defined. Several studies done previously show that GB is affected by significant ground motion amplification, up to a factor of 8, in few areas (Brax et al. 2018). They also proposed a map of the resonance frequencies within the city, showing that the frequency varies between 0.5 to 10 Hz according to the thickness of the quaternary sediments. Salloum et al. (2014) studied in a small area of GB the horizontal and vertical Vs variability in the alluvial layers using electrical tomography combined with boreholes data. They observed a high variability in the alluvial layers at a very small scale in a shallow clay layer with a thickness varying from 2 to 12 m. Moreover, they witnessed the need of combining geotechnical methods with geophysical in order to better estimate the thickness of soft layers overlying bedrock in a complex medium such as the one found in Beirut.

To achieve a comprehensive understanding of the subsoil layers and constrain the local seismic hazard in GB, this study aims to establish a 3D geotechnical model using existing and newly collected borehole data.

In recent years, 3D geotechnical modeling has emerged as a powerful tool in seismic hazard assessment, offering detailed insights into subsoil layers and their influence on seismic wave propagation (Jibson and Harp, 2002).

This research aims to analyze the lithological site effects in Greater Beirut. Initially, we will create an extensive 3D geotechnical model by combining borehole information with geophysical H/V measurements. QGIS will serve as the primary tool for analysis and visualization of this data.This approach is designed to accurately represent bedrock elevation variability of the area. The advantage of this detailed model is its enhanced capability to accurately depict how subsoil layers react to seismic events (Moss et al., 2006).

The second step of this study consists of numerical simulation of vertically incident plane wave propagation in the established 3D model. To do this, we employed advanced meshing techniques facilitated by open-source Python codes alongside the spectral-element method software, SPECFEM3D, renowned for its precision in seismic simulations and for accurately taking into account complex soil structures.

This approach not only offered a cost-effective alternative to expensive proprietary software but also significantly enhanced our efficiency. The advanced meshing technique enabled by our open-source Python codes allows for rapid generation of meshes for large and complex models. This flexibility permits efficient exploration of numerous case scenarios with different mesh sizes as needed. In this paper, we will present the methodology leading to the construction of the 3D model of Greater Beirut. We will then introduce into the main numerical simulations carried out using SPECFEM3D, starting from smooth and simple case scenarios. These first scenarios get established to ground the understanding of wave propagation within the software. Building upon such understanding, we shall subsequently apply this model to more complex, heterogeneous scenarios that characterize the area of Greater Beirut.

2. Study Area and Data Overview

2.1. Tectonic and Geological Setting

Lebanon is situated in a high seismic region between the African plate in the west and Arabian plate in the east. It is crossed by the 1000 km transform fault system known as the Levant fault system. This active fault splits into five main fault branches: the Roum, Yammouneh, Serghaya, Rachaya and Hasbaya faults as can be seen in Fig.1; this figure also illustrates the major earthquake events with the variation in magnitudes (e.g. in 551,1202,1759 and 1837).

The peninsula of Beirut advances around 10km offshore and occupies a complex wedge between Mount Lebanon and the Mediterrenean sea. Moreover, the high spatial variability of soils found in Beirut makes the small study area to be considered as a complicated geological context.

The geology of Beirut and its suburbs was described the last by Dubertret (1944). The subsoil can be categorized as quaternary deposits and rocky outcrops. The quaternary deposits, of fluvial, marine and wind origin, are composed of Brown soil with limestone pebbles, Alluvial Sand, Red Sand with and without pebbles, Cemented Dune (Ramleh) and Shifting Sand Dunes. The rock outcrops are limestone or marly limestones. Beirut features two hills in the northern part of the peninsula, about 5 km apart: Ashrafieh hill, composed of Helvetic Marls, to the east and Tallet el Khayyat hill, made of Cenomanian limestone, to the west. Both hills reach altitudes of approximately 100 meters. Furthermore, the presence of water at shallow depths in several areas of Greater Beirut significantly increases the risk of liquefaction, particularly near the River of Beirut where the water table is found at depths of 3-5 meters (Sadek et al. 2003). Mostapha et al. (2020) report that the average water table level across Greater Beirut ranges from 2m to 7m. Such conditions can lead to severe structural damage and even building collapse, posing a high risk to human safety.

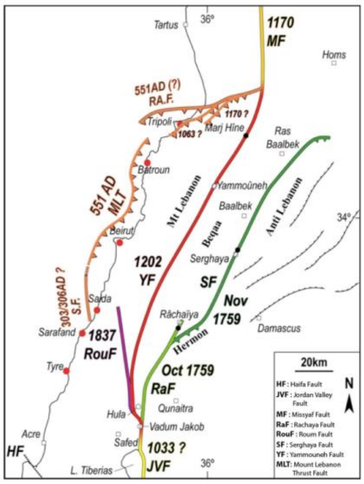

Figure 1. Map of the major faults in Lebanon with the dates of historical earthquakes. (Elias et al., 2006)

3. Methodology

3.1. Data Collection

588 geotechnical boreholes (BH) were collected from different geotechnical laboratories and design offices in order to build the 3D model for the area. The location of the boreholes is illustrated in Fig.2.

Most of the boreholes are distributed in the northern part of GB. 316 boreholes (about 53% of total number) reach the engineering bedrock where most of them are near the rocky sites.

In addition to these geotechnical data, to better limit the interpolation of the sedimentary thickness, 615 geophysical ambient vibration measurements were used and they were incorporated. These points originally reported by Brax et al. (2018) , along with additional points collected on-site during this study, will help estimate the fundamental resonance frequency (Nakamura, 1989) in each area, and will help complement the geotechnical data to reach a more robust 3D model. It is noteworthy mentioning also that the model was constrained by taking into consideration the geological map where we have outcropping rocks. In these latter zones, the bedrock elevation is indeed forced to be equal to the DEM. Moreover, high-resolution topographic data was sourced from CNRS-Lebanon, supplemented by bathymetric mapping of the Mediterranean Sea. Geological insights were gleaned from the integration of Dubertret's 1944 geological map, ensuring alignment with the topographical data's coordinate system (UTM36N).

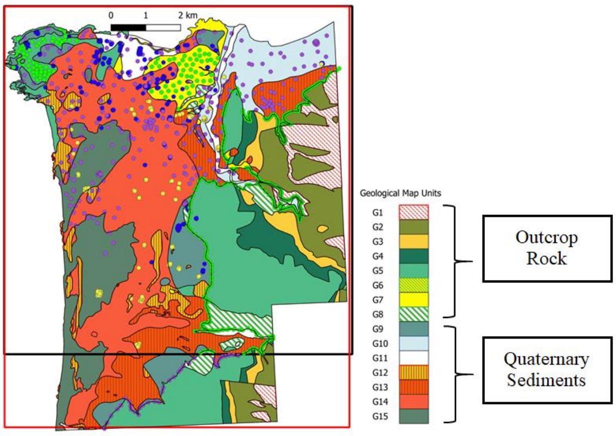

Figure 2. Geological Map of Greater Beirut with Data Points. This map delineates various geological units within the region, each color-coded to represent distinct types. Data points on the map indicate borehole locations, differentiating between those that have reached bedrock (blue dots), those that have not (yellow dots), virtual boreholes (green dots), and sites of H/V geophysical measurements (purple dots).

3.2. Data Integration Process

The process of integrating geotechnical and geophysical data into the Greater Beirut 3D model was carefully planned and executed to ensure accuracy. Our methodology involved a primary analysis to create a unified lithostratigraphic column across the region. Due to the complexity of geological units and varying sediment terminology, we adopted a two-step approach in constructing the model. Initially, we simplified the model by assuming a homogeneous sedimentary layer over the engineering bedrock. However, we planned to incorporate variations in shear wave velocity (Vs) in subsequent iterations to improve the model's accuracy. This decision was based on insights showing limited vertical Vs variability, with potential improvements guided by methods like those suggested by Tchawe et al (2021).

To estimate the Vs of the upper sediment layer, we calculated a mean velocity across the model, integrating both H/V measurements and borehole data that reached bedrock. This process utilized Nakamura's (2000) formula linking fundamental resonance frequency with sediment thickness and Vs, aiding in the standardization of data across varying geological units.

$$f_0 = \frac{V_S}{4H}$$

The integration process involved developing a quality factor (QF) system to assess the reliability of data points based on their proximity, further refined by additional fieldwork aimed at reducing distances between H/V measurements and boreholes. This approach allowed us to establish a baseline Vs_mean of 300 m/s. (Fig. 3)

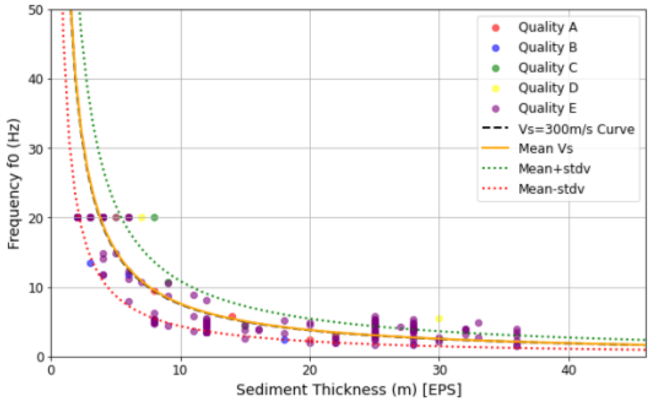

Figure 3. Frequency (f0) as a function of the thickness of sediments (EPS) before interpolating. This scatter plot is fitted by a theoretical graph of 300m/s shear wave velocity value and the lower and upper bounds of Vs to choose the best fit of the homogenized Vs-mean of the whole model chosen.

Our iterative methodology for modeling bedrock topography primarily used data from boreholes reaching bedrock and H/V points, then this preliminary surface model is compared with the minimum sediment thickness defined from boreholes not reaching bedrock, adjusting the interpolation to align with the observed constraints.

Through iterative refinements—incorporating updated data and adjusting for discrepancies—the methodology converges on a model that closely aligns with known bedrock elevations, effectively reducing uncertainties. This approach is visualized in Fig. 4, illustrating the impact of incorporating borehole data on refining the bedrock elevation model. Virtual boreholes are also utilized to address geological transitions, ensuring the model's continuity and accuracy, especially in data-sparse regions.

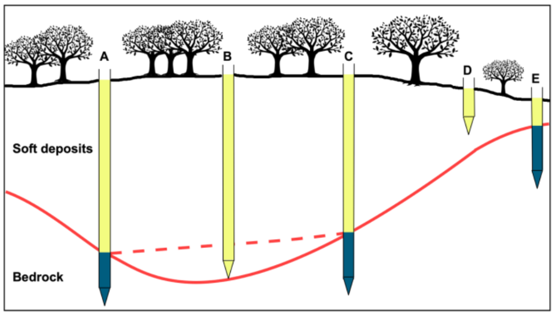

Figure 4. Illustration of the result of the iterative interpolation methodology on bedrock elevation modeling. The image displays three boreholes reaching bedrock (A,C,E) and two boreholes not reaching bedrock (B,D). The dashed line between A and C is the sediment/bedrock interface modelled without considering B. B constraints the bedrock depth to be larger and the red curve represents a more accurate interface respecting this borehole. For comparison, D doesn't constraint the interface. In this area, the final bedrock topography is similar to the one obtained with the first iteration.

3.3. Description of the 3D geotechnical model enhancement

Bedrock elevation estimation involved a detailed interpolation process, employing methods like Ordinary Kriging (OK) for their effectiveness in representing complex geological structures. OK is a preferred geostatistical approach due to its consideration of spatial variation, making it particularly effective for areas with complicated subsurface conditions and sparse data (Oliver and Webster, 2014; Chilès and Delfiner, 2012).

While Ordinary Kriging (OK) helped develop a preliminary 3D model within the area marked by the black line in Fig. 2, challenges arose in maintaining sedimentary continuity along the borders of the red rectangle as shown on the geological map. These challenges could potentially affect the accuracy of future ground motion predictions in Beirut. Thus, to construct a robust model capable of a detailed sediment layer representation, we employed a Random Forest (RF) algorithm, an AI approach renowned for its effectiveness in geotechnical studies (Breiman, 2001). This technique was chosen over continuous OK for the entire GB area due to its superior performance in data-sparse regions, particularly beneficial for addressing variogram inconsistencies of OK in the south caused by data scarcity. The RF model's adaptability to GB's unique geographical features—its coastal and mountainous terrain—further justified its application.

In our RF model, features considered for predicting bedrock elevation (ZZ_EPS) included geographical coordinates (XX as Longitude and YY as Latitude in UTM36N), distance to the coast ('tocoast'), and distance to mountains ('tomountains'). These features, chosen based on their influence on bedrock elevation within GB's geological context, were derived from the initial interpolation efforts, forming a well-constrained subset of our model selected for its high reliability and relevance to the target variable.

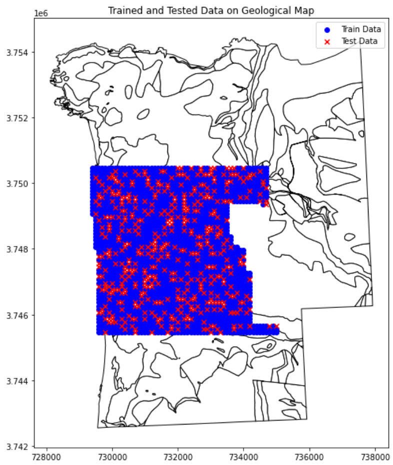

Figure 5. Data Segregation for Random Forest Training and Testing: The blue points represent the 80% of data allocated for training the model, while the red points indicate the 20% set aside for testing, illustrating the comprehensive spread of data across Greater Beirut for robust model validation.

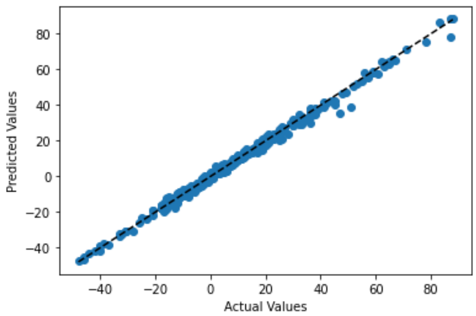

Figure 6. Predicted vs. Actual Bedrock Elevation Scatter Plot: This plot demonstrates a strong linear correlation between the model's predictions and actual bedrock elevations, underscoring the Random Forest model's precision and the fidelity of its predictions.

The performance of the RF model was assessed through partitioning the data into training and testing sets with an 80-20 split (Fig. 5), necessary for calculating the Mean Absolute Error (MAE) and assessing feature importance. This evaluation revealed model accuracy, as demonstrated by the correlation of predicted vs. actual bedrock elevation, (Fig. 6) resulting in an MAE of approximately 0.5, a Mean Squared Error (MSE) of around 2.0, and an R^2 score nearing 1.

The 3D geotechnical representation of the Greater Beirut area, delineated with a precision of 10 meters per pixel across a matrix comprising 1,225,000 individual cells, offers a detailed visualization of the bedrock elevation (Fig. 7-8). Encompassing an area of 10 kilometers by 12 kilometers, this model provides measurements of sediment thickness disparities in the whole GB area unlike previous studies, which concentrated only on the northern part of GB.

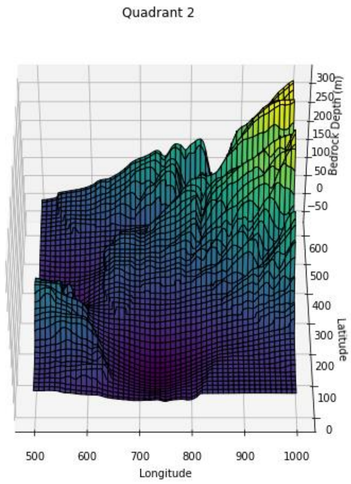

Figure 7. 3D representation of bedrock elevation across the entire study area of Greater Beirut in the easting direction.

The depths of sediments throughout the region exhibit a wide range, starting from outcropping bedrock, to exceeding 80 meters in areas presumed to be ancient riverbeds or regions with softer soils. This reveals potential zones of increased seismic vulnerability due to the likelihood of wave amplification effects. Such disparities underscore Beirut's complex geologic past and the changes in elevation from coastal to mountainous areas at a small scale. Due to this high variability in bedrock elevation, it becomes essential that we push beyond 1D techniques in analysis. As we navigate the complexities of a three-dimensional realm, seismic waves generated by an earthquake source travel and intensify within a 3D environment, ultimately reaching the surface layers in complicated patterns. This highlights the shortcomings of relying solely on 1D response analysis, as it fails to capture the complete physical dynamics of wave propagation and make precise predictions about actual ground movement (Moczo et al., 2007; Igel et al., 2015).

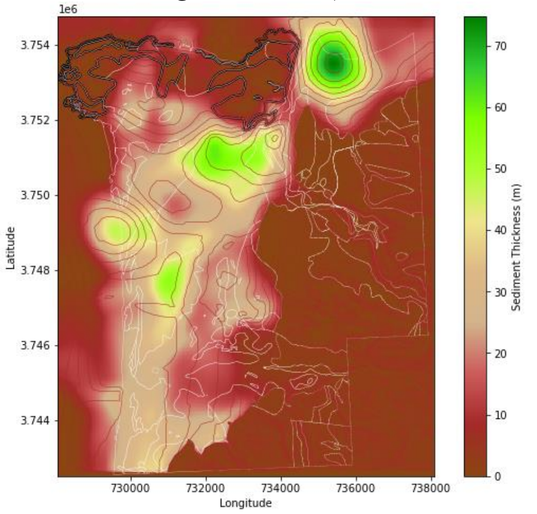

Figure 8. Sediment Thickness Variability in Greater Beirut with 10m interval contour lines of the bedrock elevation, overlaid on the geological map.

3.4. Numerical Simulations

Advanced 3D seismic simulations enable a precise representation of seismic wave propagation taking into account their interactions with diverse geological formations, as highlighted in studies by Paolucci et al. (2015), Maeda et al. (2017), Korres et al. (2022), and Tsuboi et al. (2017).

While several software packages are available for conducting these simulations, each with unique strengths tailored to specific seismic analysis aspects, SPECFEM3D emerges as the preferred option for our study. This preference is supported by its capability for GPU (Graphics Processing Unit) acceleration—a technology that utilizes the parallel processing power of GPU chips to significantly enhance simulation speeds and computational efficiency. The integration of GPU acceleration into SPECFEM3D simulations allows for handling complex and large-scale seismic data more effectively than conventional CPU-based approaches. Furthermore, our decision to employ SPECFEM3D is reinforced by the availability of an innovative, open-source Python toolkit that simplifies the mesh generation process through a non-honoring meshing technique, as documented in works by Pelties et al. (2012), Igel et al. (2015), and Touhami (2020).

3.4.1. Meshing procedure

Generating complex sub-surface geologies, particularly in regions with geometric discontinuities like basins, presents a challenge due to the difficulty in aligning the mesh with these irregularities. This issue is addressed here through a non-honouring mesh approach, where the mesh elements do not conform to the geometric discontinuities. Instead, material properties are assigned at the Gauss-Lobatto-Legendre (GLL) points within each element. This method allows for a single element to encompass varying material properties, as illustrated in the Fig. 9. The primary benefit of this technique is the significant reduction in computational costs, achieved by simplifying the mesh structure without sacrificing the simulation's accuracy.

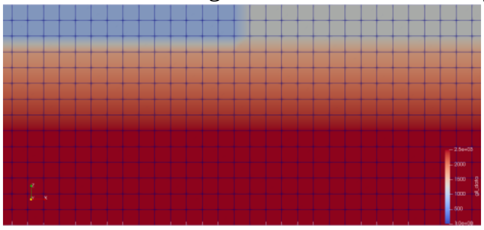

Figure 9. Non-honoring meshing technique representation

Our meshing process begins with the interpolation of topographic data to a structured grid, ensuring that the mesh conforms precisely to surface elevations and geological structures. Unlike traditional meshing tools, which often require extensive user interaction for geometry creation, mesh refinement, and topography integration, our method facilitates a "one-click" approach to generate meshes directly from topographical data files. This efficiency is achieved without sacrificing the quality or detail of the mesh, allowing for high-resolution simulations that can accommodate complex geological features (Fig. 10). This capability to quickly produce diverse meshes automatically is especially beneficial for seismic studies. It allows us to analyze wave propagation under various conditions and frequency values without manual adjustments or extensive computational resources.It allows us to explore the impact of different mesh resolutions on the accuracy and computational efficiency of seismic simulations.

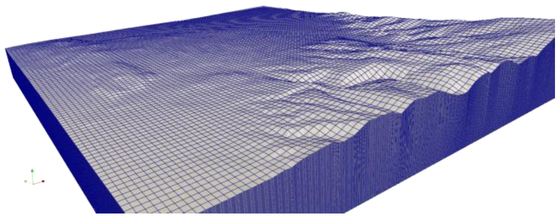

Figure 10. Representation of the meshed model for Greater Beirut

3.4.2. SPECFEM3D

SPECFEM3D is renowned for its precision in seismic simulations, making it a popular choice among seismologist researchers. For instance, Jayalakshmi et al. (2020) successfully utilized it in their study on the Indo-Gangetic basin to evaluate seismic wave amplification effects (Jayalakshmi, Dhanya, Raghukanth, & Mai, 2020). Other researchers have also demonstrated its capability in diverse geological settings, from sedimentary basins to underground mines (Wang & Cai, 2017, Van Ede et al 2019).

Despite the successful applications of SPECFEM3D in modeling seismic wave propagation, there is still a gap in using adapted source for comprehensive site effect analyses. Previous studies have indeed explored a variety of inputs, ranging from historical seismic events to moment tensor point sources (Nakano et al., 2023; Hansen et al., 2012; Chen and Romanowicz, 2023). However, the implementation of planewave sources has been less examined.

A planewave source generates seismic waves that propagate with uniform wavefronts, simulating an infinitely distant source. This characteristic makes planewave sources particularly valuable for isolating the effects of subsurface structures on seismic wave propagation, without the complexities introduced by point source or fault surface like rupture directivity or focal mechansim. The significance of representing planewave sources in SPECFEM3D lies in their ability to provide a simplified, yet effective, means of investigating site effects. Site effects refer to the modification of seismic waveforms as they travel through the Earth's uppermost crust, influenced by local geological conditions. By employing planewave sources, researchers can assess how seismic waves are amplified or attenuated by soil layers, sedimentary basins, or other geological features.

While SPECFEM3D offers the capability to couple with the new FK analysis method, this approach does not precisely align with the planewave assumptions needed in our site effect studies. The FK method, rooted in the principles of layered Earth models and the frequency-wave number domain, excels in modeling wave propagation and reflection across horizontally stratified isotropic or anisotropic materials (Capdeville et al., 2003; Coutant, 1989). It is particularly adept at handling teleseismic waves, assuming plane wave incidence to efficiently analyze how these waves interact with the Earth's subsurface layers, including the crust and upper mantle (Capdeville et al., 2003).
Acknowledging the capabilities of the software in the implementation of planewaves, and for our pursuit of applying site effect studies in (GB), we propose a methodology to replicate the effects of a planewave.

3.4.3. Implementing the plane wave input

In our study, we initially adopted a simplified approach by modeling a single force source with produced deformation propagating through a homogeneous cubic medium. This method served as an introductory step towards the implementation of plane waves (PWs) input. Upon analyzing the behavior of the single force in this homogeneous setup, we advanced our methodology by distributing this source across each node and Gauss-Lobatto-Legendre (GLL) point within the mesh at a given depth. We aim to model a vertically incident plane wave front by applying single forces evenly distributed on a horizontal plane across the mesh.This method can lead to potential discretization errors, numerical artifacts and unwanted wave reflections. These issues, as highlighted by Aki & Richards (2002), Komatitsch & Tromp (1999), and Moczo et al. (2007), may complicate the analysis by affecting the accuracy of the simulated plane wavefields and the interpretation of site effects.

To improve the accuracy and reliability of future site effect analyses in the Greater Beirut (GB) region, our efforts have been directed towards minimizing these perturbations as effectively as possible in a simple case scenario, and then applying it on GB.

3.4.4. Case scenario Configuration

The simulation scenario was constructed as a homogeneous cube with dimensions of 20km on each axis (X, Y, and Z). Utilizing the specified mesh code, the domain was discretized into hexahedral elements with a uniform mesh size of 400m. This mesh size was selected to balance the resolution with computational efficiency, considering the extensive numerical simulations required for artifact resolution. Adhering to the Nyquist criterion, the model's maximum resolvable frequency was established at 2.25Hz.

Plane wave are approximated using a series of single forces, expressed as Ricker wavelets with a central frequency of 1Hz, propagating vertically in the Z direction from predetermined depths, avoiding placing them on nodes generated from the mesh. We selected this configuration specifically to minimize the introduction of additional numerical noise, based on the considerations highlighted by Erik et al. (2020). Virtual recording stations were strategically positioned along the surface in both Northing and Easting directions, as well as vertically, extending from the surface to the model's deepest point in the center of the model. Once we've effectively reduced numerical errors, we'll use a finer mesh to capture higher frequencies. Moreover, we'll introduce horizontal forces to simulate plane S waves to assess for site effects.

3.4.5. Preliminary results of PWs implementation approximation

In our first seismic simulation within the 20km cubic model, we encountered numerical artifacts that manifested in the recorded signals, where we expected to see only the upgoing and downgoing waves as shaded in the yellow rectangle in Fig. 11. This case scenario refers to a source at depth of 9800m with a shear wave velocity (Vs) of 1800m/s and Vp over Vs ratio of 1.4. The artifacts shown in this figure is attributed to the finite distribution of forces simulating the plane wave input.

To mitigate these artifacts and refine the clarity of the main seismic signals, we implemented two key modifications that help in delaying their arrival after our interval of interest for site effects study in GB which is approximatively 10s (Youssef, 2023). First, we relocated the plane wave source to a shallower depth of 1000m, still largely below the sediment-bedrock interface in Beirut. Second, we set the Vs to 1000m/s—a value characteristic of rock sites as per Eurocodes 8. We aimed thus to delay the arrival of secondary waves as shown on Fig. 12. This adjustment resulted in a cleaner seismic section, as shown in Fig. 13, and provides a more accurate basis for site effect analysis.
Fig. 14 present the three components of the seismic motion recorded at the middle of the cube, at the surface. It shows that the motion is a pure P wave, vertically propagating. We plotted on Fig. 15 a horizontal seismic line on the surface of the cube, in the X-direction. This plot hilights in particular that the artifact waves originating from the Y-borders arrive

earlier at the stations nearest to these borders and later at the station in the center of the profile.The propagation velocity is measured close to 1000 m/s, which is equal to the S-wave velocity. We also notice that at around 13 seconds, is arriving the artifact produced at the X-borders of the cube simultaneously at all the stations of the seismic profile.

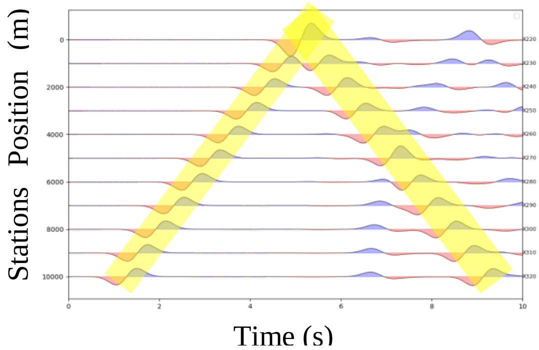

Figure 11. Seismic section for the Z component of the vertical seismic line in a 20km cubic model, source depth at 9800m, Vs=1800m/s, and source central frequency=1Hz. The uppermost station (X220) is at the surface, with stations descending at 1000m intervals to X320. The yellow shaded areas refer to the expected result; the other propagating waves refer to numerical errors.

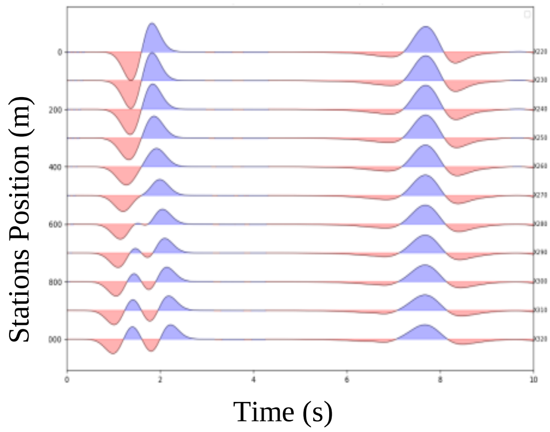

Figure 12. Vertical seismic section for the Z component in the case of the 20km cube , source depth at 1000m , Vs=1800m/s and central frequency=1Hz. Yellow shaded area refer to the expected waves, red shaded area refer to the delayed wave after relocating the source in a shallower depth.

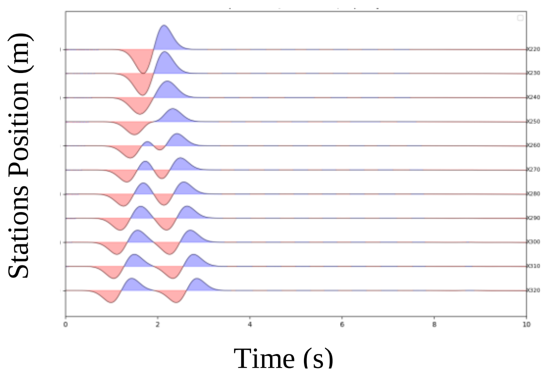

Figure 13. Vertical seismic section for the Z component in the case of the 20km cube , source depth at 1000m , Vs=1000m/s and frequency=1Hz.

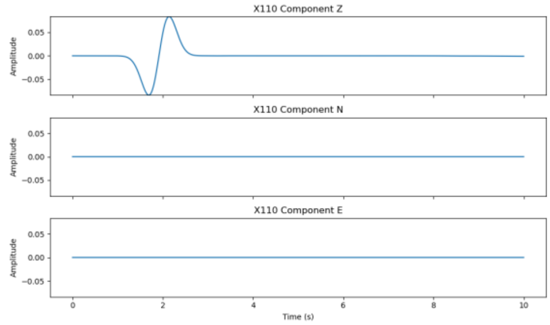

Figure 14. Three component (Z-N-E) recording of a station placed in the center and at the surface of the 20km cube model.

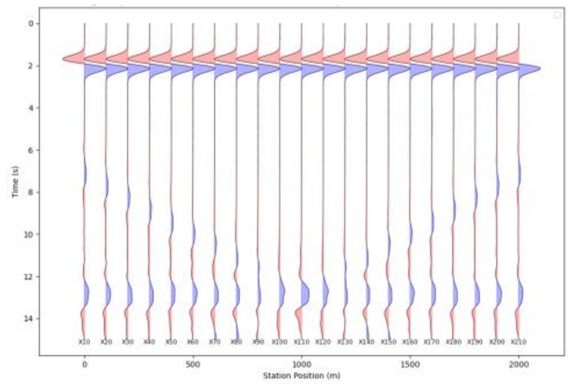

Figure 15. Seismic section for the Z component of the horizontal seismic line at the surface in the 20km cube model after resolving the artifacts faced in the first 10 seconds of the simulation.

3.4.6. Future Site effect assessment methodology in Greater Beirut

Upon establishing the method for simulating plane waves in a homogeneous cube, our next objective is to apply this technique within the Greater Beirut (GB) area. To assess the influence of topography and subsurface geology on seismic ground motion in GB, we propose a structured four-step approach. The first case scenario involves a numerical simulation, considering only a flat surface composed entirely of a homogenous medium having the properties of the bedrock. Then, the second case will follow by importing the surface topography into the model, as seen in Fig. 10, where we compare it with the recordings from the previous case. After that, we will include the homogeneous sedimentary layer, allowing us to discern the wave amplifications resulting from site effects and the presence of sediments in addition to that of the topography. The final case scenario will involve the implementation of random heterogeneities in the sediment layer.

4. Conclusion

In this study, we explored the potential for advancing seismic hazard assessment in Greater Beirut (GB) through the integration of a 3D geotechnical model, machine learning enhancements, and seismic numerical simulations. We developed the first 3D model of GB, incorporating geotechnical and geophysical data alongside geological insights. This initial interpolation approach yielded a continuous subsurface representation in the northern part of GB, though it did not extend across the entire area of interest. To address this, we employed a Random Forest algorithm to enhance the model and interpolate data in areas lacking direct measurements. Our findings highlight the variability in sediment thickness across GB, with the maximum thickness reaching approximately 80 meters.

Moreover, the application of SPECFEM3D for seismic wave propagation simulations has introduced a level of precision and computational efficiency, particularly with the adoption of the non-honoring meshing technique specified for this study. Ultimately, we successfully simulated planewave propagations using SPECFEM3D's capabilities and addressed challenges related to unwanted wave reflections and numerical artifacts by adjusting parameters to achieve cleaner outputs. This will facilitate risk analysis in GB and future numerical simulations in the region.

Acknowledgements

Authors would like to acknowledge the National Council for Scientific Research of Lebanon (CNRS-L), the Agence Universitaire de la Francophonie (AUF) and Gustave Eiffel University for the doctoral fellowship.

References

• Books

Breiman, L. (2001). "Random Forests." Machine Learning, 45, pp. 5-32. https://doi.org/10.1023/A:1010933404324

Chilès, J.P., and Delfiner, P. (2012). "Geostatistics: Modeling Spatial Uncertainty." Wiley Series in Probability and Statistics.

Dubertret, L. (1945). "Geologie du site de Beyrouth: avec carte geologique au 1/20.000." Delegation Generale de France Combattant Au Levant.

Igel, H. (2017). Computational Seismology: A Practical Introduction. Oxford University Press.

Koene, E. F. M., Robertsson, J. O. A., & Andersson, F. (2020). "A consistent implementation of point sources on finite-difference grids." Geophysical Journal International, 223(2), pp. 1144–1161. https://doi.org/10.1093/gji/ggaa383

Moczo, P., Robertsson, J. O. A., & Eisner, L. (2007). "The Finite-Difference Time-Domain Method for Modeling of Seismic Wave Propagation." In R. Wu, V. Maupin, & R. Dmowska (Eds.), Advances in Geophysics (Vol. 48, pp. 421-516). Elsevier. ISBN 9780120188505. https://doi.org/10.1016/S0065-2687(06)48008-0.

• Journal articles

Brax, M., Bard, P.Y., Duval, A.M., et al. (2018). "Towards a microzonation of the Greater Beirut area: an instrumental approach combining earthquake and ambient vibration recordings." Bulletin of Earthquake Engineering, 16, pp. 5735–5767. https://doi.org/10.1007/s10518-018-0438-1

Elias, A., Tapponnier, P., Singh, S. C., King, G. C. P., Briais, A., Daëron, M., Carton, H., Sursock, A., Jacques, E., Jomaa, R., & Klinger, Y. (2007). "Active thrusting offshore Mount Lebanon: Source of the tsunamigenic A.D. 551 Beirut-Tripoli earthquake." Geology, 35(8), pp. 755–758. https://doi.org/10.1130/G23631A.1

Faccioli, E., Paolucci, R., & Vanini, M. (2015). "Evaluation of Probabilistic Site-Specific Seismic-Hazard Methods and Associated Uncertainties, with Applications in the Po Plain, Northern Italy." Bulletin of the Seismological Society of America, 105(5), pp. 2787–2807. https://doi.org/10.1785/0120150051

Harp, E. L., & Jibson, R. W. (2002). "Anomalous Concentrations of Seismically Triggered Rock Falls in Pacoima Canyon: Are They Caused by Highly Susceptible Slopes or Local Amplification of Seismic Shaking?." Bulletin of the Seismological Society of America, 92(8), pp. 3180–3189. https://doi.org/10.1785/0120010171

Jayalakshmi, S., Dhanya, J., Raghukanth, S. T. G., & Mai, P. M. (2020). "3D seismic wave amplification in the Indo-Gangetic basin from spectral element simulations." Soil Dynamics and Earthquake Engineering, 129, article id. 105923. https://doi.org/10.1016/j.soildyn.2019.105923

Korres, M., Lopez-Caballero, F., Fernandes, V. A., Gatti, F., Zentner, I., et al. (2023). "Enhanced seismic response prediction of critical structures via 3D regional scale physics-based earthquake simulation." Journal of Earthquake Engineering, 27(3), pp. 546-574. https://doi.org/10.1080/13632469.2021.2009061. HAL Id: hal-03424424.

Maeda, T., Takemura, S., & Furumura, T. (2017). "OpenSWPC: an open-source integrated parallel simulation code for modeling seismic wave propagation in 3D heterogeneous viscoelastic media." Earth, Planets and Space, 69, 102. https://doi.org/10.1186/s40623-017-0687-

Moss, R. E., Seed, R. B., Kayen, R. E., Stewart, J. P., Der Kiureghian, A., & Cetin, K. O. (2006). "CPT-Based Probabilistic and Deterministic Assessment of In Situ Seismic Soil Liquefaction Potential." Journal of Geotechnical and Geoenvironmental Engineering, 132(8). https://doi.org/10.1061/(ASCE)1090-0241(2006)132:8(1032)

Nakamura, Y. (1989). "A Method for Dynamic Characteristics Estimation of Subsurface Using Microtremor on the Ground Surface." Railway Technical Research Institute, Quarterly Reports, 30(1), pp. 25-33. Available at: http://www.rtri.or.jp/eng/.

Oliver, M. A., & Webster, R. (2014). "A tutorial guide to geostatistics: Computing and modelling variograms and kriging." Catena, 113, pp. 56-69. https://doi.org/10.1016/j.catena.2013.09.006

Pelties, C., de la Puente, J., Ampuero, J.-P., Brietzke, G. B., & Käser, M. (2012). "Three-dimensional dynamic rupture simulation with a high-order discontinuous Galerkin method on unstructured tetrahedral meshes." First published: 18 February 2012. https://doi.org/10.1029/2011JB00885

Salloum, N., Jongmans, D., Cornou, C., Abdel Massih, D. Y., Hage Chehade, F., Voisin, C., & Mariscal, A. (2014). "The shear wave velocity structure of the heterogeneous alluvial plain of Beirut (Lebanon): combined analysis of geophysical and geotechnical data." Geophysical Journal International, 199(2), pp. 894-913. https://doi.org/10.1093/gji/ggu294

Tsuboi, S., Ando, K., Miyoshi, T., Peter, D., Komatitsch, D., & Tromp, J. (2016). "A 1.8 trillion degrees-of-freedom, 1.24 petaflops global seismic wave simulation on the K computer." The International Journal of High Performance Computing Applications, 1–12. https://doi.org/10.1177/1094342016632596. Reprints and permissions: sagepub.co.uk/journalsPermissions.nav

van Ede, M.C., Molinari, I., Imperatori, W., et al. (2020). "Hybrid Broadband Seismograms for Seismic Shaking Scenarios: An Application to the Po Plain Sedimentary Basin (Northern Italy)." Pure and Applied Geophysics, 177, pp. 2181–2198. https://doi.org/10.1007/s00024-019-02322-

• Dissertations/Theses

Youssef, Eliane (2023) “Simulation of the seismic response in complex media: accounting for the soil spatial variability using non-stationary random fields and application to Beirut city (Lebanon).”